International Journal of Modern Physics B

HELIUM IN PORES AND IRREGULAR SURFACES

E. S. HERNÁNDEZ

Departmento de Física, Facultad de Ciencias Exactas y Naturales, Universidad de Buenos Aires and CONICET, 1428 Buenos Aires, Argentina
shernand@df.uba.ar

A. HERNANDO, R. MAYOL and M. PI

Departament d'Estructura i Components de la Matèria, Facultat de Física, Universidad de Barcelona and IN², E-808028 Barcelona, Spain
alberto@ecm.ub.es,ricardo@ecm.ub.es,marti@ecm.ub.es

Received Day Month Year
Revised Day Month Year

We report studies of adsorption of helium in translationally invariant polygonal pores at zero temperature, with emphasis on the route to capillary condensation and the appearance of metastable states. We analyze hysteresis and hysterectic–like phenomena associated to the existence of multiple equilibrium states in a rhombic pore and examine the effects of the angular geometry, as opposed to the smooth curvature of cylindrical tubes.

Keywords: helium; confinement; hysteresis

1. Introduction

The current research focuses upon adsorption of helium inside nanopores and on real surfaces which are not flat within the atomic scale. It is well known that imperfections on a physical adsorber such as steps, stripes, cavities and grooves give rise to corrugation and roughness, which modify the thermodynamics and dynamics of wetting with respect to a planar surface. In particular, recent experiments[1,2] of wetting of superfluid ^{4}He on rough Cs show memory effects and hysterectic dynamics of the contact line, attributed to the persistence of filled micropuddles after dewetting. Although planar Cs and cesiated surfaces are known to be heliophobic at temperatures below 2 K, the presence of cavities limits Cs heliophobicity, as is the case *i.e.*, in the interior of hollow spheres and cylinders[3] and at the inner angle of planar wedges.[4] It is a general characteristic of confinement potentials that a concave curvature or angle increases the adatom-adsorber attraction and may change heliophobicity into heliophilicity. A similar enhancement of the adhesive forces could be expected in the case of an irregular Cs surface, for which a simplified model consists of a collection of heliophilic sites on a heliophobic surface, as realized in a recent

experiment[5] of adsorption of hydrocarbon liquids on silicon surfaces patterned with an array of parabolic nanocavities.

Our present project and emerging studies include, as a first step, adsorption of helium in translationally invariant polygonal pores, that is expected to give rise to capillary condensation (CC) with adsorption–desorption branches arranged into a hysteresis loop, as for classical fluids. The interest of polygonal pores lies in the presence of angles, which permit the appearance of density distributions with either high or low symmetry. The latter implies the simultaneous appearance of various meniscus shapes, which can be associated to drops and bubbles on the walls, in contrast with the much simpler configurations that show up in the popular cylindrical tubes. Furthermore, we intend to investigate adsorption of He on planar Cs at finite temperatures, involving the construction of adsorption isotherms with subsequent appearance of metastability and instability regions, and adsorption of He in finite pores on a flat surface at nonvanishing temperatures, that would originate changes in the wetting-prewetting phase diagram with respect to the case of a perfect planar adsorber.

In this report we provide a brief account of the current state–of–the–art regarding adsorption of classical fluids in nanopores (section 2) and in section 3 we describe our calculations and results, which are summarized in section 4.

2. Classical fluids in nanopores

Although nanoporous materials have been used since antiquity as adsorbents and filters, the industrial production of activated carbon began in 1900 and of zeolites around 1950 and today various processes permit to manufacture porous materials with multiple chemical, geological and geophysical, and industry applications. Very useful reviews on production, classification, uses, and topics of general interest regarding nanopores can be found in Refs. 6, 7. In general, one refers to these environments as micropores if their diameter D is below 2 nm, mesopores if D is between 2 and 50 nm, and macropores for diameters larger than 50 nm. The adsorption sequence of a fluid in a pore permits one to identify two clearly different regimes or "phases", namely a low–density, vapor–like configuration where a thin layer of fluid adheres to the inner walls, and a high–density, liquid–like one with the fluid homogeneously condensed in the tube, corresponding to CC.

A well studied phenomenon occurring along the CC regime of the adsorption isotherm is hysteresis. In addition to abundant experimental evidence, a very clear picture of hysteresis can be attained by means of Monte Carlo simulations as reported for example in Ref. 8. The classical explanation of this phenomenon goes back as far as 1911 [9] and received stronger support in 1938,[10] with simple thermodynamic arguments that permit to relate the adsorption and desorption pressures to the saturation properties of the unconfined fluid. The general understanding is that the vapor pressure at the adsorption branch is close to the spinodal pressure of vapor in the pore, while the lower desorption pressure is that of liquid–gas coex-

istence under confinement. However, this simple scenario can be strongly modified by the geometry of the pore and/or the pore array.

Studies of CC of classical fluids have been performed employing various techniques such as grand canonical and canonical Monte Carlo simulations, nonlocal density functionals, lattice gas models, molecular dynamics and other methods.[6,11] In particular, it has been proven that nonlocal density functional theory (NLDFT), which has been applied to pore physics for more than 20 years, with appropriate choice of the force parameters provides results in excellent agreement with both simulations and experiments for CC in nanopores,[11] and bridges the gap between simulations carried on pores of around 2 nm diameter and the thermodynamic limit. It is important to note that a well-known feature of both theory and experiments of classical fluids in pores, that has been already discussed at length in the literature,[6] is the possible existence of multiple metastable states with grand potential above the equilibrium value at a given fluid density. according to the choice of the initial condition. This is the basis for the appearance of hysterectic loops, although such features may also show up below the CC regime, under proper choice of the initial condition for the construction of the mass distribution.

In this work, we concentrate on adsorption of superfluid helium in polygonal pores, as predicted by a specific NLDFT described *i.e.*, in Ref. 4 and refs. cited therein. Previous studies by our group[12,13] have undertaken hexagonal pores, for which calculations based in rigorous many-body techniques exist in the literature. However, these approaches make use of a rather crude approximation for the confinement potential, such as the summation of the planar Lenard–Jones potentials of six planes meeting at angles of sixty degrees. Here we consider a rhombic pore, an environment that can be regarded as a double–wedge and has been investigated from various viewpoints. On the one hand, a symmetry–breaking localization–delocalization transition of the liquid–vapor interface in a double wedge has been identified.[14]. Moreover, we have shown that helium in wedges can adopt various meniscus shapes[4] and that helium samples adsorbed near a corner grow with accumulation of quasi–onedimensional stripes.[15] Finally, rhombic pores, which appear naturally in mineral crystals and are manufactured in metallic and organic materials since the 60's,[16] have been realized experimentally.[17] The rhombic pore is then a simple and feasible candidate to investigate a variety of aspects of the morphology and the thermodynamics of adsorption in a tube, such as the coexistence of different meniscus shapes at the smallest and the largest angle, the competition of quasi–onedimensional stripes and quasi–twodimensional layers in the process of filling, and the sensitivity of the equilibrium density profile to the initial condition, among others.

3. Calculations and results

Our calculations employ grand canonical NLDFT for superfluid helium at zero

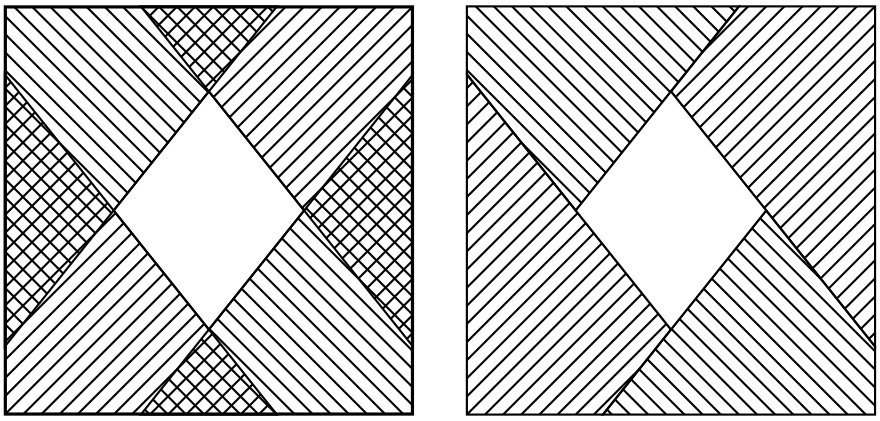

Fig. 1. Left panel: Four half–solids meeting at corners to form a rhombic cavity, overlapping at the vertices. Right panel: Same environment created by four nonoverlapping cusps.

temperature, which amounts to solving a nonlinear Schrödinger–like equation for the twodimensional density profile $\rho(x,z)$ (we assume the pore infinity along the y–axis) of the form

$$\left[-\frac{\hbar^2}{2m}\nabla^2 + U(\rho) + U(x,z)\right]\sqrt{\rho(x,z)} = \mu\sqrt{\rho(x,z)} \tag{1}$$

Here $U(\rho)$ is the mean field potential described by the density functional, $U(x,z)$ the adsorbing potential of the pore walls and μ the chemical potential of the helium atoms. The density is normalized to a fixed number of particles per unit length $n = N/L$.

In earlier descriptions of polygonal pores and walls meeting at a corner, the adsorbing potential has been approximated by summing the contributions from infinite planar surfaces. In this context, four half-solids make a rhombic pore with strong overlap at the vertices –thus overestimating the strength of the confinement– as indicated with the doubly hatched regions in the left panel of Fig. 1. In a recent paper[18] we have shown that this approach can be substantially improved by solving first an inverse problem: in fact, given a planar potential $U_{ref}(z)$, it is possible to find a pair potential or source field $V(\mathbf{r}-\mathbf{r}')$ such that the reference field is the convolution

$$U_{ref}(z) = \rho_0 \int_{-\infty}^{0} dz' \int\int dx'dy'\, V(\mathbf{r}-\mathbf{r}') \tag{2}$$

For a half-solid with bulk density ρ_0, one finds the exact solution

$$V(z) = \frac{U''_{ref}(z)}{2\pi\rho_0 z} \tag{3}$$

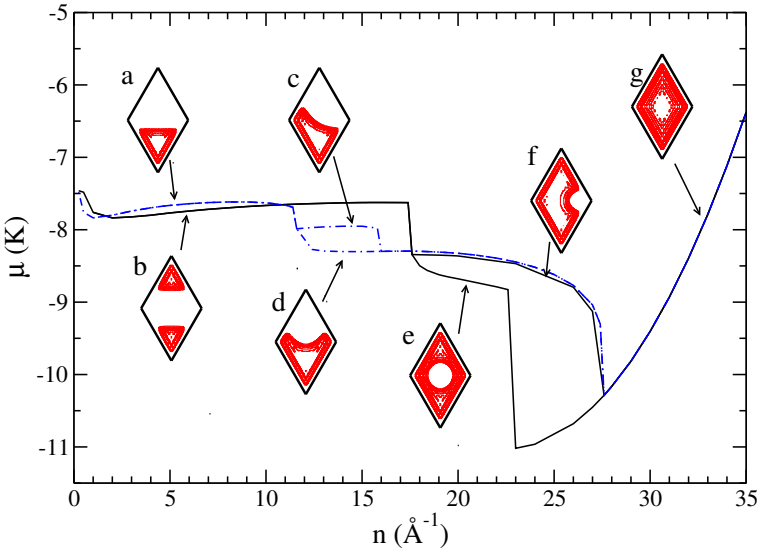

Fig. 2. Grand potential per particle Ω/N along the proposed paths (see text for details) in full and dashed–dotted lines, respectively, in a rhombic Cs pore with small angle of 60° and 50 Å side. The insets (a) to (g) have been respectively drawn for linear densities n = 9, 9, 12, 16, 20, 26 and 29 Å^{-1}. The arrows point to the path (not to the value of n).

so that for other matter distributions $n(\mathbf{r}')$ one can compute

$$U(\mathbf{r}) = \int d\mathbf{r}'\, n(\mathbf{r}')\, \frac{U''_{ref}(|\mathbf{r}-\mathbf{r}'|)}{2\pi\rho_0|\mathbf{r}-\mathbf{r}'|} \tag{4}$$

As shown in Ref. 18, a convenient, infinite unit cell is the cusp, –*i. e.*, the complement of a wedge– for which the adsorbing field $U(\mathbf{r})$ can be computed out of the potential for a plane using Eq. (4). A rhombic pore can thus be viewed as surrounded by four nonoverlapping cusps, as illustrated in the right panel of Fig. 2.

We have computed the equation of state (EOS) for helium atoms in a rhombic Cs mesopore with sides of 50 Å and small angle of 60°, solving Eq. (1) by means of an imaginary–time evolution technique, whose details can be found in Ref. 4 and refs. cited therein. The adsorption field $U(\mathbf{r})$ has been obtained from the planar *ab–initio* potential U_{ref} for Cs developed in Ref. 19. The outcome of these calculations is usually presented as a zero–temperature isotherm $\Omega(n)$ where $\Omega = E/L - \mu n$ is the grand potential per unit length, or as an isotherm of the form $\mu(n)$. At finite temperatures, the latter can be related to the experimental adsorption isotherms, generally expressing the vapor pressure as a function of the amount of adsorbed material.

The appearance of hysteresis and hysterectic–like loops can be due to two different situations. One can construct adsorption and desorption branches by a step–by–step procedure that computes smooth changes in Ω, μ and the mass distribution

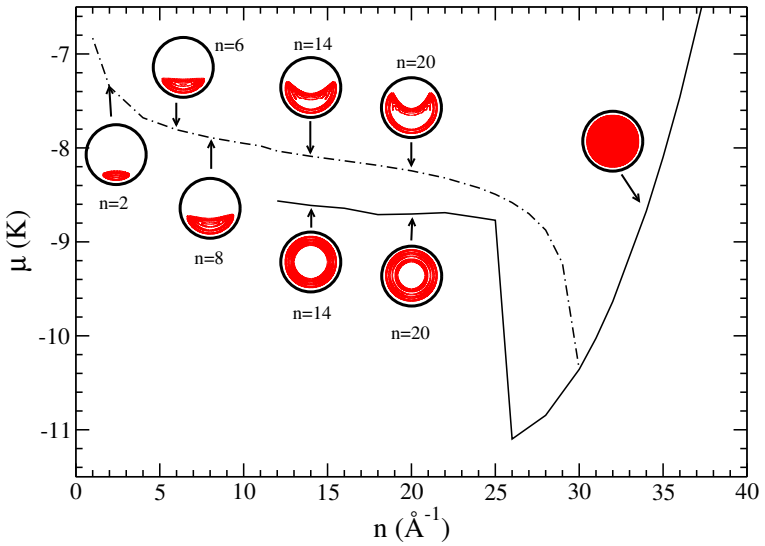

Fig. 3. Same as Fig. 2 for a cylinder with the same transverse area as the rhombic pore.

due to small variations in the linear density n, giving rise to "true" hysteresis. As an alternative, one can evolve different initial density distributions for a fixed linear density. In this case it is possible to find multiple equilibrium configurations; if this happens, examination of the grand potential permits to identify the thermodynamic equilibrium states and the metastable states.

In Fig. 2 we illustrate the curves $\mu(n)$ obtained by imaginary–time evolution of two different initial conditions, with the insets depicting the equilibrium density profiles in the tube. Configurations (a), (d), (c) and (f) correspond to an initial mass distribution with helium filling uniformly the lower half–pore, while patterns (b) and (e) are obtained from the fluid filling the whole pore. These two trajectories merge together at a linear density near 28 Å^{-1}, showing that for larger helium samples the fluid is capillary condensed in the pore according to profile (g).

The stability analysis by observation of the grand potential Ω shows that stable thermodynamic equilibrium does not always correspond to the configuration with the highest symmetry.[13]. Typical symmetry–breaking patterns such as (c) and (d) have been generated by adding noise to the initial steps of the imaginary–time evolution and are thermodynamically unstable. For the lowest densities the mass distribution, either stable or metastable, represents fluid located on the pore walls. The crossing at the two trajectories at 17.5 Å^{-1} for a chemical potential of -8.5 K is the vapor–like endpoint of a Maxwell construction with rightmost end at 32.5 Å^{-1}. Within this density range both the high and low symmetry patterns are thermodynamically unstable, while for higher densities the fluid is capillary condensed in a stable fashion. We note that although configurations (e) and (g) are similar in

appearance, only the latter corresponds to CC with a central density close to bulk saturation, while the former contains a central void.

The behavior above described can be contrasted with the equivalent zero–temperature isotherms for a cylindrical tube with the same transverse area, plotted in Fig. 3. In this case the amount of symmetry–breaking is reduced, due to the absence of corners which precludes patterns like (c) and (f) in Fig. 2; moreover, a high symmetry pattern like (b) in the rhombic pore does not occur in the cylindrical tube. One can recognize as well that the density distributions in the cylinder are of type (a) and (d) at the lowest linear densities, while the configurations for $n =$ 14 and 20 Å^{-1} present a bubble at the center, similar to the rhombic distribution (e). The lowest branch, that resembles the adsorption curve in a true adsorption isotherm, contains the cylindrically symmetric configurations, while those with broken symmetry can be associated to the desorption branch.

4. Summary and perspectives

In this paper we have reported studies of adsorption of helium in (translationally invariant) polygonal pores at zero temperature, with emphasis on CC and appearance of metastable states. We believe that at the moment we possess the appropriate instruments to study and understand the road to CC, with accompanying hysteresis and hysterectic–like phenomena associated to the existence of multiple equilibrium states in a pore.

We plan to carry finite temperature calculations of adsorption isotherms on a heliophobic Cs surface, employing a temperature–dependent density functional, previous to undertaking a more stringent investigation of adsorption on a rough surface. Since these isotherms present instability regions (*i.e.* $d\mu/dn < 0$) an important phenomenon that deserves further investigation is nucleation and cavitation of helium in the presence of a wall. We hope to present these results in the near future, as well as those of adsorption of He in finite pores on a flat surface, pointing at examining the changes in the wetting-prewetting phase diagram due to the presence of interfacial irregularities.

Acknowledgements

This work has been performed under grants FIS2005-01414 from DGI, Spain (FEDER), 2005SGR00343 from Generalitat de Catalunya and in Argentina, PIP 5138/05 from CONICET, PICT 31980/05 from ANPCT and X298 from University of Buenos Aires.

1. J. Klier, P. Leiderer, D. Reinelt and A. F. G. Wyatt, *Phys. Rev. B* **72**, 245410 (2005)
2. D. Reinelt, V. Iov, P. Leiderer and J. Klier, *J. Phys.: Condens. Matter* **17**, S403 (2005)
3. L. Szybisz and S. M. Gatica, *Phys. Rev. B* **64**, 224523 (2001).
4. E. S. Hernández, F. Ancilotto, M. Barranco, R. Mayol and M. Pi, *Phys. Rev. B* **73**, 2454061 (2006)

5. O. Gang, K. J. Alvine, M. Fukuto, P. S. Pershan, C. T. Black and B. M. Ocko, *Phys. Rev. Lett.* **95**, 217801 (2005)
6. L. D. Gelb, K. E. Gubbins, R. Radhakrishnan and M. Sliwinska-Bartkowiak, *Rep. Prog. Phys.* **62**, 1573–1659 (1999)
7. E. Robens, P. Staszczuk, A. Dabrowsky and M. Barczak, *J. Thermal Analysis and Calorimetry* **79**, 499 (2005)
8. L. D. Gelb, *Molec. Phys.* **100**, 2049 (2002); R. Paul and H. Rieger, *J. Chem. Phys.* **123**, 024708 (2005).
9. R. Zigsmondy, *Z. Anorg. Chem.* **71**, 356 (1911).
10. L. H. Cohan, *J. Am. Chem. Soc.* **60**, 433 (1938).
11. A. V. Neimark, P. I. Ravikovitch and A. Vishnyakov, *Phys. Rev. E* **62**, R1493 (2000)
12. E. S. Hernández, A. Hernando, R. Mayol and M. Pi, *Proceedings of the 14th International Conference on Recent Progress in Many–Body Theory*, Barcelona, Spain, July 2007, eds. G. Astrakharchik, J. Boronat and F. Mazzanti, to be published.
13. A. Hernando, E. S. Hernández, R. Mayol and M. Pi, submitted for publication.
14. A. Milchev, M. Müller, K. Binder and D. P. Landau, *Phys. Rev. Lett.* **90**,136101 (2003)
15. R. Mayol, F. Ancilotto, M. Barranco, E. S. Hernández and M. Pi, *J. Low Temp. Phys.***148**, 851 (2007)
16. M. A. M. Beerlage, J. M. M. Peeters, J. A. M. Nolten, M. H. V. Mulder and H. Strathmann, *J. Appl. Pol. Sci.* **75**, 1180 (1999); R. G. Harrison, N. K.Dally, and A. Y. Nazarenko, *Chem. Commun.* 1387 (2000); S. Matthias, F. Müller, and U. Gösele, *J. Apl. Phys.* **98**, 023524 (2005).
17. P. F. McKenzie, R. M. Weber and J. L. Anderson,*Langmuir* **10**, 1539 (1994)
18. A. Hernando, E. S. Hernández, R. Mayol and M. Pi, *Phys. Rev. B* **76**, 1154291 (2007)
19. A. Chizmeshya, M. W. Cole, and E. Zaremba, *J. Low Temp. Phys.* 110, 677 (1998).